Hydrogen/Deuterium Isotope Effects on the NMR Chemical Shifts and Geometries of Intermolecular Low-Barrier Hydrogen-Bonded Complexes

Sergei N. Smirnov,[1a,b] Nikolai S. Golubev,*[,1a,b] Gleb S. Denisov,*[,1b] Hans Benedict,[1a] Parwin Schah-Mohammedi,[1a] and Hans-Heinrich Limbach*[,1a]

Contribution from the Institut für Organische Chemie, Takustrasse 3, Freie Universität Berlin, D-14195 Berlin, FRG, and Institute of Physics, St. Petersburg State University, 198904 St. Petersburg, Russian Federation

Received October 12, 1995[⊗]

Abstract: In this paper we describe H/D isotope effects on the chemical shifts of intermolecular hydrogen-bonded complexes exhibiting low barriers for proton transfer, as a function of the position of the hydrogen bond proton. For this purpose, low-temperature (100−150 K) ^{1}H, ^{2}H, and ^{15}N NMR experiments were performed on solutions of various protonated and deuterated acids AL (L = H, D) and pyridine-^{15}N (B) dissolved in a 2:1 mixture of $CDClF_2$/CDF_3. In this temperature range, the regime of slow proton and hydrogen bond exchange is reached, leading to resolved NMR lines for each hydrogen-bonded species as well as for different isotopic modifications. The experiments reveal the formation of 1:1, 2:1, and 3:1 complexes between AH(D) and B. The heteronuclear scalar ^{1}H−^{15}N coupling constants between the hydrogen bond proton and the ^{15}N nucleus of pyridine show that the proton is gradually shifted from the acid to pyridine-^{15}N when the proton-donating power of the acid is increased. H/D isotope effects on the chemical shifts of the hydrogen-bonded hydrons (proton and deuteron) as well as on the ^{15}N nuclei involved in the hydrogen bonds were measured for 1:1 and 2:1 complexes. A qualitative explanation concerning the origin of these low-barrier hydrogen bond isotope effects is proposed, from which interesting information concerning the hydron and heavy atom locations in single and coupled low-barrier hydrogen bonds can be derived. Several implications concerning the role of low-barrier hydrogen bonds in enzyme reactions are discussed.

Introduction

The nature of low-barrier hydrogen bonds is an old problem of experimental and theoretical chemistry.[2] The interest in this problem has recently been revived because of the presumed role of these bonds during emzyme catalysis.[3] Therefore, all techniques which can give novel information on low-barrier hydrogen bonds are of importance. One method which has not yet been fully exploited is nuclear magentic resonance (NMR) spectroscopy. By using NMR of organic solids, novel information concerning the dynamics of proton and deuteron transfer in weak as well as moderately strong hydrogen-bonded systems has been obtained.[4] Recently, this method has also been applied to the case of low-barrier hydrogen bonds embedded in the solid state.[5] In this paper, we describe new NMR stratagems for the study of low-barrier hydrogen bonds in the liquid state. The first stratagem is based on performing experiments in the temperature range between 100 and 120 K using special solvents.[3o,6] Under these conditions, various hydrogen-bonded complexes can then be observed in slow exchange within the NMR time scale. The solvents employed consist of liquified, deuterated compounds which are gaseous at room temperature, e.g. a freonic mixture such as $CDClF_2$/CDF_3. The second

⊗ Abstract published in *Advance ACS Abstracts,* April 1, 1996.

(1) (a) Free University of Berlin. (b) St. Petersburg State University. Presented at the Summer School on Isotope Effects as Tools in Basic and Environmental Research, University of Roskilde, Denmark, June 24−28, 1995, and the ACS Symposium "Proton Transfer", Chicago, August 20−24, 1995.

(2) (a) Schuster, P., Zundel, G., Sandorfy, C., Eds. *The Hydrogen Bond;* North Holland Publ. Co.: Amsterdam, 1976. (b) Kreevoy, M. M.; Liang, T. M. *J. Am. Chem. Soc.* **1980**, *102*, 361. (c) Emsley, J.; Jones, D. J.; Lucas, J. *Rev. Inorg. Chem.* **1981**, *3*, 105. (d) Ault, B. S. *Acc. Chem. Res.* **1982**, *15*, 103. (e) Mootz, D.; Bartmann, K. *Angew. Chem.* **1988**, *100*, 424; *Angew. Chem., Int. Ed. Engl.* **1988,** *27*, 391. (f) Berthold, H. J.; Preibsch, E.; Vonholdt, E. *Angew. Chem.* **1988**, *100*, 1581; *Angew. Chem., Int. Ed. Engl.* **1988**, *27*, 1527. (g) Hibbert, F.; Emsley, J. *Adv. Phys. Org. Chem.* **1980**, *26*, 255. (h) Novak, A. *Struct. Bonding (Berlin)* **1974**, *18*, 177.

(3) (a) Swain, C. G.; Kuhn, D. A.; Schowen, R. L. *J. Am. Chem. Soc.* **1965**, *87*, 1553. (b) Eliason, R.; Kreevoy, M. M. *J. Am. Chem. Soc.* **1978**, *100*, 7037. (c) Cleland, W. W.; Kreevoy, M. M. *Science* **1994**, *264*, 1887. (d) Perrin, C. L. *Science* **1994**, *266*, 1665. (e) Blow, D. M.; Birktoft, J. J.; Hartley, B. S. *Nature* **1969**, *221*, 337. (f) Blow, D. M.; Steitz, T. A. *Annu. Rev. Biochem.* **1970**, *39*, 63. (g) Hadzi, D. *J. Mol. Struct.* **1988**, *177*, 1. (h) Schowen, R. L. In *Mechanistic Principles of Enzyme Activity*; Liebman, J. F., Greenberg, A., Eds.; VCH Publishers: New York, 1988; p 119. (i) Schowen, K. B.; Schowen, R. L. *Methods Enzymol.* **1982**, *87*, 551. (j) Venkatasubban, K. S.; Schowen, R. L. *CRC Crit. Rev. Biochem.* **1984**, *17*, 1. (k) Cook, P. F. *Enzyme Mechanisms from Isotope Effects*; CRC Press: New York, 1992. (l) Frey, P. A.; Whitt, S. A.; Tobin, J. B. *Science* **1994**, *264*, 1927. (m) Denisov, G. S.; Golubev, N. S.; Gindin, V. A.; Limbach, H. H.; Ligay, S. S.; Smirnov, S. N. *J. Mol. Struct.* **1994**, *322*, 83. (n) Golubev, N. S.; Gindin, V. A.; Ligay, S. S.; Smirnov, S. N. *Biochemistry (Moscow)* **1994**, *59*, 447. (o) Golubev, N. S.; Smirnov, S. N.; Gindin, V. A.; Denisov, G. S.; Benedict, H.; Limbach, H. H. *J. Am. Chem. Soc.* **1994**, *116*, 12055. Huskey, W. P. *J. Am. Chem. Soc.*, submitted.

(4) (a) Limbach, H. H. Dynamic NMR Spectroscopy in the Presence of Kinetic Isotope Effects. In *NMR Basic Principles and Progress*; Springer: Berlin, 1991; Vol. 26, Chapter 2. (b) Smith, J. A. S.; Wehrle, B.; Aguilar-Parrilla, F.; Limbach, H. H.; Foces-Foces, M. C.; Cano, F. H.; Elguero, J.; Baldy, A.; Pierrot, M.; Khurshid, M. M. T.; Larcombe-McDuall, J. B. *J. Am. Chem. Soc.* **1989**, *111*, 7304. (c) Schlabach, M.; Wehrle, B.; Braun, J.; Scherer, G.; Limbach, H. H. *Ber. Bunsen-Ges. Phys. Chem.* **1992**, *96*, 821. (d) Braun, J.; Schlabach, M.; Wehrle, B.; Köcher, M.; Vogel, E.; Limbach, H. H. *J. Am. Chem. Soc.* **1994**, *116*, 6593. (e) Aguilar-Parilla, F.; Scherer, G.; Limbach, H. H.; Foces-Foces, M. C.; Cano, F. H.; Smith, S. A. S.; Toiron, C.; Elguero, J. *J. Am. Chem. Soc.* **1992**, *114*, 9657. (f) Hoelger, Ch.; Wehrle, B.; Benedict, H.; Limbach, H. H. *J. Phys. Chem.* **1994**, *98*, 843.

(5) (a) Hoelger, Ch.; Limbach, H. H *J. Phys. Chem.* **1994**, *98*, 11803. (b) Benedict, H.; Hoelger, Ch.; Aguilar-Parrilla, F.; Fehlhammer, W. P.; Wehlan, M.; Janoschek, R.; Limbach, H. H. *J. Mol. Struct.*, in press.

(6) (a) Denisov, G. S.; Golubev, N. S. *J. Mol. Struct.* **1981**, *75*, 311. (b) Golubev, N. S.; Bureiko, S. F.; Denisov, G. S. *Adv. Mol. Relax. Inter. Proc.* **1982**, *24*, 225. (c) Golubev, N. S.; Denisov, G. S.; Pushkareva, E. G. *J. Mol. Liq.* **1983**, *26*, 169. (d) Golubev, N. S.; Denisov, G. S. *J. Mol. Struct.* **1992**, *270*, 263.

S0002-7863(95)03445-7 CCC: $12.00

stratagem consists of performing NMR experiments on complexes partially deuterated in the mobile proton sites. Therefore, because of the slow hydrogen bond exchange, it becomes possible to detect hydrogen/deuterium isotope effects on NMR chemical shifts of intermolecular low-barrier hydrogen-bonded systems. These isotope effects contain interesting information on the hydrogen bond properties. So far, with exception of the very strong FHF^-/FDF^- hydrogen bond,[7] we are only aware of isotope effects on chemical shielding of intramolecular hydrogen bonds.[8]

Since we were looking for a series of neutral hydrogen-bonded complexes with different proton locations as models for snapshots of proton transfer, we decided to study a variety of organic acids interacting with pyridine. A number of spectroscopic investigations have been carried out on these compounds.[9] In a preliminary low-temperature NMR study, we showed recently that acetic acid forms not only 1:1 complexes with pyridine-^{15}N in $CDClF_2/CDF_3$ but also 2:1 and 3:1 complexes which exchange slowly on the NMR time scale at 110 K.[3o] The values of the intrinsic proton chemical shifts and the scalar coupling constant $^1J_{^1H-^{15}N}$ indicated a proton displacement toward pyridine as the number of acetic acid molecules increased. In this paper, we describe H/D isotope effects on the intrinsic chemical shifts of the nuclei involved in the low-barrier hydrogen bonds between several acids and pyridine-^{15}N using low-temperature ^1H, ^2H, and ^{15}N NMR, from which some interesting qualitative conclusions about the hydrogen bond geometries can be obtained.

This paper is organized as follows. After a short experimental section, a general section is included in which the origin of H/D isotope effects on chemical shielding is discussed in a qualitative way, with a special emphasis on low-barrier hydrogen bonds. The effects of H/D substitution in the mobile proton sites of hydrogen-bonded complexes between acids and pyridine in freonic solutions at low temperature are then described and discussed.

Experimental Section

All experiments reported in this paper were performed on a 500 MHz Bruker NMR spectrometer AMX 500; the deuterated freon solvent mixture $CDClF_2/CDF_3$ (2:1) freezes below 90 K. It was synthesized as described previously[3o] at 100 °C and elevated pressures (between 30 and 60 bar) from $CDCl_3$ via fluorination with $SbF_3/SbCl_5$, a modification of the recipe proposed by Siegel et al.[10] The solvent was handled on a vacuum line which also served to prepare the samples using well-established techniques.[4a] Its composition was checked by NMR. Pyridine-^{15}N (95% enriched) was purchased from Chemotrade, Leipzig, Germany.

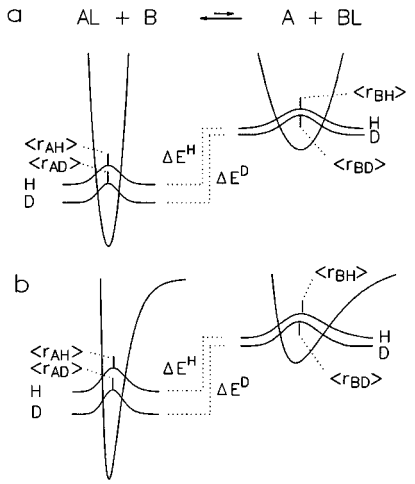

Figure 1. Origin of H/D isotope effects on chemical shifts of two-atomic molecules AL (L = H, D). Vibrational states are represented by the squares of the corresponding wave functions positioned at the corresponding energy. Average positions are symbolized by small vertical lines. (a) No intrinsic isotope effect on the chemical shifts arises in the case of the harmonic oscillator because the average distances $\langle r_{AH}\rangle$ and $\langle r_{AD}\rangle$ are equal. Due to the different zero-point energies in AL and BL, the energy differences, i.e. equilibrium constants of the tautomerism, are different for the protonated and the deuterated systems.[11] (b) In the anharmonic case, $\langle r_{AH}\rangle$ is larger than $\langle r_{AD}\rangle$ and an intrinsic isotope effect on the chemical shift arises. Equilibrium isotope effects are superimposed to the intrinsic effects.

General Section

In the past, two kinds of H/D isotope effects on chemical shifts of proton transfer systems have been discussed, i.e. intrinsic and equilibrium isotope effects,[7] as illustrated in Figure 1. Intrinsic isotope effects are induced by changes of molecular geometries via H/D substitution, whereas equilibrium isotope effects arise from isotopic fractionation between different sites[11] which interconvert rapidly in the NMR time scale. In this section we firstly discuss the origin of both effects and then describe H/D isotope effects on low-barrier hydrogen bonds representing an intermediate between the intrinsic and equilibrium isotope effects.

Equilibrium H/D Isotope Effects on Chemical Shifts. The occurrence and the theory of equilibrium isotope effects[11] mainly arising from mass effects on zero-point energies are well-known. The vibrational contribution is schematically illustrated in Figure 1a for the simplest case of slowly exchanging diatomic

(7) Fujiwara, F. Y.; Martin, J. S. *J. Am. Chem. Soc.* **1974**, *96*, 7625.

(8) (a) Gunnarson, G.; Wennerström, H.; Egan, W.; Forsén, S. *J. Am. Chem. Soc.* **1978**, *100*, 8264. (b) Hansen, P. E. Isotope Effects in Nuclear Shielding. *Prog. NMR Spectrosc.* **1988**, *20*, 207. (c) Hansen, P. E. *J. Mol. Struct.* **1994**, *321*, 79. (d) Hansen, P. E.; Lycka, A. *Acta Chem. Scand.* **1989**, *43*, 222. (f) Hansen, P. E.; Kawecki, R.; Krowczynski, A.; Kozerski, L. *Acta Chem. Scand.* **1990**, *44*, 836. (g) Munch, M.; Hansen, A. E.; Hansen, P. E.; Bouman, T. D. *Acta Chem. Scand.* **1992**, *46*, 1065. (h) Hansen, P. E.; Christoffersen, M.; Bolvig, S. *Magn. Reson. Chem.* **1993**, *31*, 893.

(9) For references concerning properties of pyridine−carboxylic acid complexes see: (a) Zeegers-Huyskens, Th.; Huyskens, P. *Molecular Interactions*; J. Wiley & Sons: Chichester, U.K., 1980; Vol. 2, p 1. (b) Zundel, G.; Fritsch, J. In *The Chemical Physics of Solvation*; Dogonadze, R. R., Kálmán, E.; Kornyshev, A. A.; Ulstrap, J., Eds.; Elsevier: Amsterdam, **1986**; Vol. 38B, p 21. (c) Dega-Szafran, Z.; Szafran, M. *Heterocycles* **1994,** *37*, 627. (d) Lindemann, R.; Zundel, G. *J. Chem. Soc., Faraday Trans. 2* **1972**, *68*, 979. (e) *Ibid.* **1990**, *86*, 301. (f) Dega-Szafran, Z.; Hrynio, A.; Szafran, M. *J. Mol. Struct.* **1990**, *240*, 159. (g) Gusakova, G. V.; Denisov, G. S.; Smolyanski, A. L.; Schreiber, V. M. *Dokl. Akad. Nauk. SSSR* **1970**, *193*, 1065. (h) Dega-Szafran, Z.; Grunwald-Wyspianska, M.; Szafran, M. *Spectrochim. Acta* **1991**, *47A*, 125. Sobczyk, L. *J. Mol. Struct.*, **1988**, 177, 111. (i) Dega-Szafran, Z.; Dulewicz, E. *J. Chem. Soc., Perkin Trans. 2* **1983,** 345. (k) Dega-Szafran, Z.; Grunwald-Wyspianska, M.; Szafran, M. *J. Chem. Soc., Faraday Trans.* **1991**, *87*, 3825. (l) Odinokov, S. E.; Mashkovsky, A. A.; Glazunov, V. P.; Iogansen, A. V.; Rassadin, B. V. *Spectrochim. Acta* **1976**, *322A*, 1355. (m) Glazunov, A. V. P.; Mashkovsky, A.; Odinokov, S. E. *Spectrosc. Lett.* **1976**, *9*, 391. (n) Odinokov, S. E.; Nabiullin, A. A.; Mashkovsky, A. A.; Glazunov, V. P. *Spectrochim. Acta* **1983**, *39A*, 1055. (o) Jerzykiewicz, L. B.; Lis, T.; Malarski, Z.; Grech, E. *J. Crystallogr. Spectosc. Res.* **1993**, *23*, 805.

(10) Siegel, J. S.; Anet, F. *J. Org. Chem.* **1988**, *53*, 2629.

(11) (a) Bigeleisen, J.; Wolfsberg, M. *Adv. Chem. Phys.* **1958**, *1*, 15. (b) More O'Ferrall, R. A. *Substrate Isotope Effects*, in *Proton Transfer Reactions*; Caldin, E. F., Gold, V., Eds.; Chapman and Hall: London, **1975**; Chapter 8, p 201−262. (c) Bone, R.; Wolfenden, R. *J. Am. Chem. Soc.* **1985**, *107*, 4772. (d) Chiang, Y.; Kresge, A. J.; Chang, T. K.; Powell, M. F.; Wells, J. A. *J. Chem. Soc., Chem. Commun.* **1995**, 1587. (e) Loh, S. N.; Markley, J. L. *Biochemistry* **1994**, *33*, 1029−1036. (f) Arrowsmith, C. H.; Guo, H. X.; Kresge, J. *J. Am. Chem. Soc.* **1994**, *116*, 8890. (g) Shiner, V. J., Jr.; Neumann, T. E. *Z. Naturforsch*. **1989**, *44a*, 337−354. (h) Jarret, R. M.; Saunders, M. *J. Am. Chem. Soc.* **1985**, *107*, 2648. (i) Baltzer, L.; Bergman, N. A. *J. Chem. Soc., Perkin Trans. 2* **1982**, 313. (j) Gold,V.; Grist, S. *J. Chem. Soc. B* **1971**, 1665. (k) Gold, V.; Tomlinson, C. *J. Chem. Soc. B* **1971**, 1707. (l) Al-Rawi, J. M. A.; Bloxsidge, J. P.; Elvidge, J. A.; Jones, J. R.; More O'Ferrall, R. A. *J. Chem. Soc., Perkin Trans 2*, **1979**, 1593. (m) Salomaa, P. *Acta Chem. Scand.* **1969**, *23*, 2095. (n) Jencks, W. P.; Salvesen, K. *J. Am. Chem. Soc.* **1971**, *93*, 4433.

molecules AH + B ⇄ A + BH and AD + B ⇄ A + BD, characterized by the equilibrium constants $K^H = x_{BH}x_A/x_{AH}x_B$ and $K^D = x_{BD}x_A/x_{AD}x_B$. If the vibrations are harmonic, the squares of the vibrational wave functions, i.e. the probability of finding a hydron L = H, D at a given location, are very similar. In particular, the average hydron positions $\langle r_{AH}\rangle$ and $\langle r_{AD}\rangle$ are equal, as illustrated in Figure 1a by vertical bars. The average chemical shifts of AH and AD will therefore also be similar, i.e. intrinsic H/D isotope effects on chemical shifts are absent. When the hydron is transferred to the base B, the force constant of the B−H stretching vibration may be smaller, as shown on the right-hand side of Figure 1a, leading to a reduction of the zero-point energies. Figure 1a thus explains why the equilibrium constant K^H is larger than K^D. In the case of fast proton transfer, the average chemical shift of a nucleus i = A, B, H, D in the system is given by

$$\delta_i = \frac{1}{K^L - 1}\delta_i(\text{AL or B}) + \frac{K^L}{K^L - 1}\delta_i(\text{A or BL}), \qquad L = H, D \quad (1)$$

where δ_i(AL or B) and δ_i(A or BL) represent the intrinsic chemical shifts of i in the different molecules. Since $K^H > K^D$, δ_i will be different for L = H and D. It will moreover strongly depend on temperature because of the temperature dependence of K^L. Finally, we note that an equilibrium constant $K = K^D/K^H$ can be defined for the equilibrium AD + BH ⇄ AH + BD. This constant is generally called the "fractionation factor".[11]

Intrinsic H/D Isotope Effects on Chemical Shifts. If the potential is anharmonic as indicated in Figure 1b, the proton and deuteron wave functions and their squares are substantially different, leading to a larger value for $\langle r_{AH}\rangle$ as compared to $\langle r_{AD}\rangle$. Therefore, intrinsic H/D isotope effects on the chemical shifts of the nuclei studied will result, as chemical shielding is strongly dependent on the nuclear geometries. In principle, the intrinsic isotope effects are independent of temperature as long as vibrational excitation and other temperature-dependent changes of the nuclear geometry are negligible. Generally, only the sum of equilibrium and intrinsic isotope effects can be measured. According to the literature[8b] one defines

$$^p\Delta H(D) = \delta(A\underline{H}) - \delta(A\underline{D}) \quad (2)$$

as the "primary" H/D isotope effect, i.e. the chemical shift difference between the proton and the deuteron.

$$^n\Delta A(D) = \delta(\underline{A}H) - \delta(\underline{A}D) \quad (3)$$

represents the chemical shift difference of nucleus A in the protonated and the deuterated molecule. Usually, the superscript *n* refers to the number of covalent chemical bonds between the observed nucleus A and the site of isotopic substitution. Throughout this paper, we treat intermolecular hydrogen-bonded complexes like single molecules and include in *n* also the intermolecular hydrogen bonds.

Low-Barrier Hydrogen Bond H/D Isotope Effects on Chemical Shifts. In the case of low-barrier hydrogen bonds between an acid AL and a base B, it is very difficult to know whether H/D isotope effects on chemical shifts are caused by intrinsic or equilibrium isotope effects. Consider for example the simplest case of a linear 1:1 hydrogen-bonded complex between an acid AL and a base B. We label the distance between A and L as r_1 and the distance between L and B as r_2, and neglect the bending vibration. The potential energy $V(r_1,r_2)$ of the nuclear motion is not harmonic and contains anharmonic coupling terms.[2] A typical two-dimensional potential energy surface is depicted schematically in Figure 2, where we use as coordinates the sum $r_1 + r_2$ and the difference $r_1 - r_2$. $r_1 + r_2$ is the distance between the two heavy atoms of the hydrogen bond. $r_1 - r_2$ is a natural coordinate describing the progress of proton transfer. If $r_1 - r_2 < 0$ the proton is near A, at $r_1 + r_2 = 0$ in the center between A and B, and at $r_1 + r_2 > 0$ near B. It is possible to calculate the two-dimensional vibrational wave functions and their squares $\Psi^2_{A-L\cdots B}(r_1-r_2,r_1+r_2)$ according to the literature[12] and the average nuclear positions. Such a calculation would show that even in the vibrational ground state the geometries of A−D···B and A−H···B are different. In particular, the average value $\langle r_1+r_2\rangle_D$ will be larger than $\langle r_1+r_2\rangle_H$. On the other hand, $\langle r_1-r_2\rangle_H$ will be less negative than $\langle r_1-r_2\rangle_D$. In other words, the heavy atom distance between A and B is larger in A−D···B than in A−H···B, but the distance between A and D of the covalent bond is shorter than between A and H as indicated schematically in Figure 2. The increase of the distance between A and B upon deuteration was observed experimentally in a number of crystalline salts by Ubbelohde[14a] and has been studied theoretically by several authors.[14b,c]

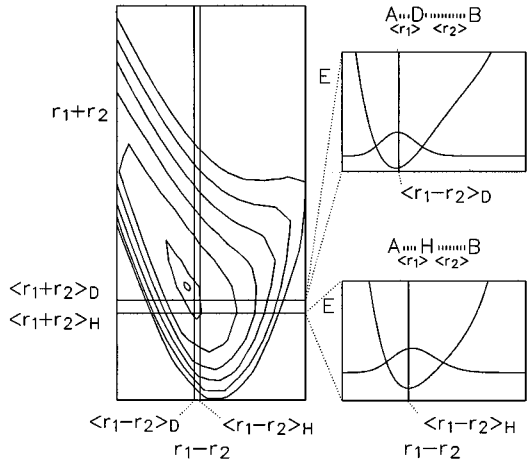

Figure 2. Contour plot of a two-dimensional potential energy surface of the hydron L = H, D motion in a linear hydrogen-bonded complex A−L···B as a function of the variables $r_1 - r_2$ and $r_1 + r_2$. The two-dimensional vibrational wave functions not shown lead to different average proton and deuteron distances $\langle r_1-r_2\rangle_L$ and $\langle r_1+r_2\rangle_L$ as indicated. On the right side, the one-dimensional projections including the wave functions for the average values $\langle r_1+r_2\rangle_D$ (top) and $\langle r_1+r_2\rangle_H$ (bottom) are shown.

The one-dimensional potential functions and the one-dimensional vibrational square functions or hydron density distribution functions $\Psi^2_{A-L\cdots B}(r_1-r_2)$ in the groundstate at the fixed average heavy atom distances $\langle r_1+r_2\rangle_D > \langle r_1+r_2\rangle_H$ are slightly different for A−H···B and A−D···B, as depicted on the right-hand side of Figure 2, but this result does not mean a different total potential energy surface for both species. In conclusion, when H is replaced by D, the smaller heavy atom−hydron distance decreases but the larger distance increases even more, leading to a widening of the hydrogen bond. When bending vibrations are included, this Ubbelohde effect may be more complicated and even reverse.[14]

(12) (a) Somorjai, R. L.; Hornig, D. F. *J. Chem. Phys.* **1962**, *36*, 1980. (b) Janoschek, R.; Weidemann, E. G.; Pfeiffer, H.; Zundel, G. *J. Am. Chem. Soc.* **1972**, *94*, 2387.

(13) (a) Steiner, Th.; Saenger, W. *Acta Crystallogr.* **1994**, *B50*, 348. (b) Steiner, Th. *J. Chem. Soc., Chem. Commun.* **1995**, 1331. (c) Gilli, P.; Bertolasi, V.; Ferretti, V.; Gilli, G. *J. Am. Chem. Soc.* **1994**, *116*, 909.

(14) (a) Ubbelohde, A. R.; Gallagher, K. G. *Acta Crystallogr.* **1955**, *8*, 71. (b) Legon, A. C.; Millen, D. J. *Chem. Phys. Lett.* **1988,** *147*, 484. (c) Sokolov, N. D.; Savel'ev, V. A. *Chem. Phys.* **1977**, *22*, 383. (d) Sokolov, N. D.; Savel'ev, V. A. *Chem. Phys.* **1994**, *181*, 305.

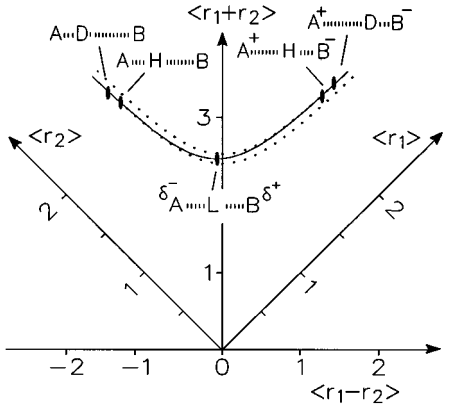

Figure 3. Correlation between the average hydrogen bond distances $\langle r_1 \rangle$ and $\langle r_2 \rangle$ in Å, according to eq 4, adapted from refs 13. This correlation implies an equivalent correlation between the proton transfer reaction coordinate $\langle r_1 - r_2 \rangle \approx \langle r_1 \rangle - \langle r_2 \rangle$ and the average heavy atom distance $\langle r_1 + r_2 \rangle \approx \langle r_1 \rangle + \langle r_2 \rangle$. In the case where A ≡ oxygen and B ≡ nitrogen, the quasi-midpoint where the minimum of $\langle r_1 + r_2 \rangle$ occurs is realized at $\langle r_1 \rangle < \langle r_2 \rangle$, where the proton is closer to oxygen than to nitrogen. The dotted lines indicate the correlations of Steiner et al.[13a,b] for O−H···O (top line) and N−H···N (bottom line) hydrogen-bonded systems.

The question now arises as to how the hydrogen bond geometry and the isotope effects on this geometry change when the proton is transferred from A to B, i.e. when the zwitterionic complex is formed. This transfer may be achieved by various means, e.g. the increase of the acidity of the proton donor or the basicity of the acceptor, a change of the solvent polarity, temperature, etc. A qualitative answer to this problem can be obtained by correlations of Steiner et al.[13a,b] and Gili et al.[13c] between the two average distances $\langle r_1 \rangle$ and $\langle r_2 \rangle$ of a number of neutron crystal structures containing O···H···O (A, B = O) and N···H···N (A, B = N) hydrogen bonds.[13] A similar correlation can be expected for the less symmetric O···H···N (A = O, B = N) hydrogen-bonded systems. By interpolation from the O···H···O and N···H···N data of Steiner et al.,[13a,b] one can easily derive the equation

$$\langle r_2 \rangle \approx \langle r_2^\circ \rangle - b_2 \ln\{1 - \exp[(\langle r_1^\circ \rangle - \langle r_1 \rangle)/b_1]\} \qquad (4)$$

where $\langle r_1^\circ \rangle$ and $\langle r_2^\circ \rangle$ represent the average OH and NH distances in the absence of hydrogen bonding and $b_i = \{[\langle r_1 + r_2 \rangle_{min} - 2\langle r_i^\circ \rangle]/\ln 4\}$. $\langle r_1 + r_2 \rangle_{min}$ represents the minimum average heavy atom distance. The correlation between $\langle r_1 \rangle$ and $\langle r_2 \rangle$ according to eq 4 is depicted in Figure 3. This signifies that an increase of the acidity of AH which increases the average distance $\langle r_1 \rangle$ is accompanied by a decrease of the distance $\langle r_2 \rangle$. In a way similar to that discussed above, the difference $\langle r_1 - r_2 \rangle \approx \langle r_1 \rangle - \langle r_2 \rangle$ is the reaction coordinate representing in a series of complexes AHB the progress of the average proton positions. $\langle r_1 - r_2 \rangle$ is negative for the molecular complex A-H···B and positive for the zwitterionic complex $A^-\cdots H-B^+$. The complementary variable is then the heavy atom distance $\langle r_1 + r_2 \rangle \approx \langle r_1 \rangle + \langle r_2 \rangle$. The correlation of eq 4 then signifies a contraction of the hydrogen bond during the transfer of the proton from A to B. In the symmetric O···H···O and N···H···N bonds, the contraction is maximal at $\langle r_1 \rangle = \langle r_2 \rangle$, but in the case of the O···H···N bonds the shortest hydrogen bond is realized at $\langle r_1 - r_2 \rangle < 0$, where the distance between O and H is smaller than between H and N,[13] as illustrated in Figure 3. In the following we call this point the "quasi-midpoint".

By introducing the results of Figure 2 into Figure 3, it immediately becomes evident that the distance between A and L decreases when H is replaced by D in the molecular complex

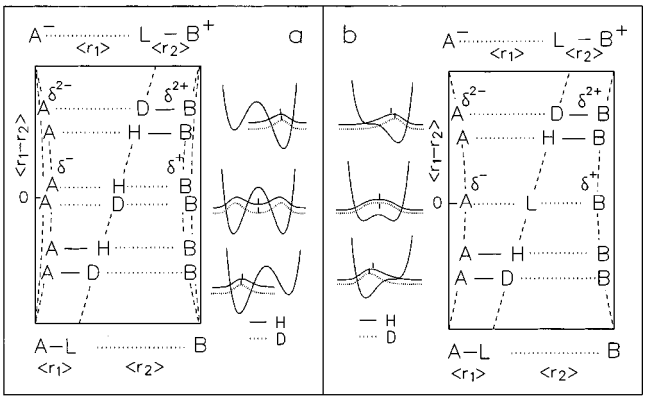

Figure 4. One-dimensional hydron (L = H, D) potentials and geometric changes during the transfer of a hydron from A to B characterized by the reaction coordinate $\langle r_1 - r_2 \rangle$. The squares of the wave functions of the vibrational ground states for H and D, i.e. the proton and deuteron distribution functions, are included; however, for the sake of clarity, the difference in the one-dimensional potential functions for H and D according to Figure 2 is omitted. (a) A barrier at the quasisymmetric midpoint leads to a small H/D isotope effect on the geometry absent in the case (b) with a very low barrier.

and increases in the zwitterionic form. In both cases the distance between A and B increases. Therefore, at the quasi-midpoint, only a small or even no geometric H/D isotope effect is expected. Some experimental[5b] and theoretical evidence[15] exists for the absence of geometric isotope effects at least in the case of extremely small or absent barriers for the proton motion.

The geometric changes associated with an increase of the acidity of AH and with deuteration can also be plotted schematically in a reaction path diagram as indicated in Figure 4 where the associated one-dimensional potential functions and the proton and deuteron density distribution functions in the vibrational ground state are included. The absence of a geometric isotope effect at the quasi-midpoint is evident in Figure 4b as the proton and deuteron density distribution functions are similar. By contrast, in the case of a symmetric double well, the functions are different and the proton is on average located closer to the hydrogen bond center than the deuteron as indicated in Figure 4a; consequently, a widening of the hydrogen bond is expected in the case of a double well.

Results

1:1 Complexes of Carboxylic Acids with Pyridine-^{15}N. In Figure 5, some low-temperature NMR spectra of samples of AH *o*-toluic acid (a−c) and of 2-thiophenecarboxylic acid (d−f) in the presence of a small excess of pyridine-^{15}N dissolved in $CDClF_2/CDF_3$ (2:1) are shown. The deuterium fraction in the mobile proton sites was about 80%. Under the conditions employed, hydrogen bond exchange is slow on the NMR time scale. The signals of the H-bond protons are split into doublets by scalar coupling with ^{15}N. The coupling constant $^1J_{^1H-^{15}N}$ is relatively small (12 Hz) in the case of *o*-tolylic acid as proton donor, indicating that the proton is preferentially localized near A, but is much larger (57 Hz) in the case of 2-thiophenecarboxylic acid, indicating that the proton is located near B.

(15) Almlöf, J. *Chem. Phys. Lett.* **1972**, *17*, 49.
(16) (a) Witanowski, M.; Stefaniak, L.; Webb, G. A. *Annual Reports on NMR Spectroscopy, 11 B*; Academic Press: New York, 1981. (b) Martin, G.; Martin, M. L.; Gouesnard, J. P. *NMR-Basic Principles and Progress*; Springer: Heidelberg, Germany, 1989; Vol. 18 *(^{15}N NMR Spectroscopy)* and references cited therein.
(17) (a) *Handbook of Chemistry and Physics, 63rd ed.;* CRC Press Inc.: Boca Raton, FL, 1982−1983. (b) Kortüm, G.; Vogel, W.; Angrussow, K. *Dissociation constants of organic acids in aqueous solution*; London: Butterworths, 1961.

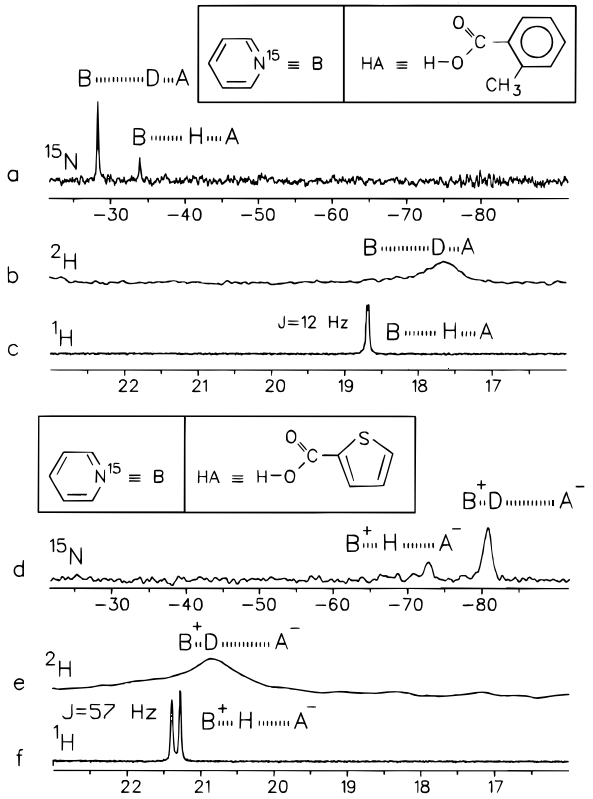

Figure 5. ^{15}N NMR (a, d), ^{2}H NMR (b, e), and ^{1}H NMR (c, f) spectra (^{1}H Larmor frequency 500.13 MHz) of solutions of pyridine-^{15}N (B) and carboxylic acids (AL, L = H, D) in a 2:1 mixture of $CDClF_2$/CDF_3 at a deuterium fraction in the mobile proton sites $D = 0.8$. (a−c) 125 K, $C_B = 0.033$ M, $C_{AH} + C_{AD} = 0.028$ M. (d−f) 110 K, $C_B = 0.045$ M, $C_{AH} + C_{AD} = 0.035$ M. The ^{15}N chemical shifts are referred to internal free pyridine, where $\delta(CH_3NO_2) = \delta(C_5H_5N) - 69.2$ ppm and $\delta(NH_4Cl) = \delta(CH_3NO_2) - 353$ ppm.[16]

2-Thiophenecarboxylic acid, therefore, has a greater acidity or proton donating power in comparison to *o*-toluic acid. Moreover, the hydrogen bond is longer in the case of *o*-toluic acid compared to 2-thiophenecarboxylic acid, as indicated by the low-field shift from 18.68 to 21.33 ppm. The ^{2}H NMR spectra (Figure 5b,e) of the same samples reveal primary upfield isotope shifts $^{p}\Delta H(D) = \delta(A\underline{H}B) - \delta(A\underline{D}B)$ for the hydrogen bond hydron of about +1 ppm in the case of *o*-toluic acid and of +0.5 ppm in the case of 2-thiophenecarboxylic acid, indicating that in both cases the hydrogen bond is weakened. The ^{15}N spectra give interesting additional information. Firstly, hydrogen bonding and proton transfer to pyridine leads to a high-field shift of the pyridine ^{15}N signal, where the chemical shift scale of Figure 5 refers to the absorption of free pyridine. These high-field shifts are in accordance with the increase of $^{1}J_{^{1}H-^{15}N}$. However, in the 80% deuterated samples, two lines appear where the more intense line arises from the deuterated complexes ADB and the smaller line from AHB which are in slow exchange. We observe that the one-bond isotope effect across the hydrogen bond, $^{n}\Delta^{15}N(D) = {}^{1}\Delta^{15}N(D) = \delta(AH\underline{B}) - \delta(AD\underline{B})$, is negative in the case of *o*-toluic acid, where $n = 1$ signifies the hydrogen bond, but positive in the case of 2-thiophenecarboxylic acid, where $n = 1$ signifies a covalent bond between ^{15}N and the hydron.

Qualitatively, these effects can be explained in terms of Figures 2−4. In both cases, the hydrogen bond is widened upon deuteration, as expressed in a positive primary H/D isotope effect $^{p}\Delta H(D) = \delta(A\underline{H}) - \delta(A\underline{D}) > 0$. In the case of the molecular complex A−H···B, where AH ≡ *o*-toluic acid, the distance between the hydron and the ^{15}N is increased by deuteration, leading to a negative value $^{1}\Delta^{15}N(D) = \delta(AH\underline{B}) - \delta(AD\underline{B}) < 0$; on the other hand, in the case of the zwitterionic complex $A^- \cdots H{-}B^+$, where AH ≡ 2-thiophenecarboxylic acid, the distance between the ^{15}N nucleus and the hydron is decreased by deuteration, leading to a positive value of $^{1}\Delta^{15}N(D)$.

The results of a series of measurements where the acid AL was varied in a wide range are assembled in Table 1 and depicted in Figure 6. The ^{15}N chemical shift $\delta^{15}N$ is conveniently used as a measure of the proton transfer coordinate $\langle r_1 - r_2 \rangle$ from the acid to pyridine. When the proton-donating power of AH is increased, the hydrogen bond proton signal shifts to low field, goes through a maximum, and then shifts back again to high field. At the same time, the scalar coupling constant $^{1}J_{^{1}H-^{15}N}$ increases from almost 0 to about 90 Hz. The dependence of the primary isotope effects $^{p}\Delta H(D)$ as a function of $\delta^{15}N$ is always positive but contains two maxima of unequal height. The one-bond isotope effect on $^{1}\Delta^{15}N(D)$ exhibits a dispersion-like structure. We note that the all chemical shifts and isotope effects are independent of concentration but dependent on temperature; however, it is remarkable that temperature variations lead only within the margin of error to shifts along the solid lines in Figure 6.

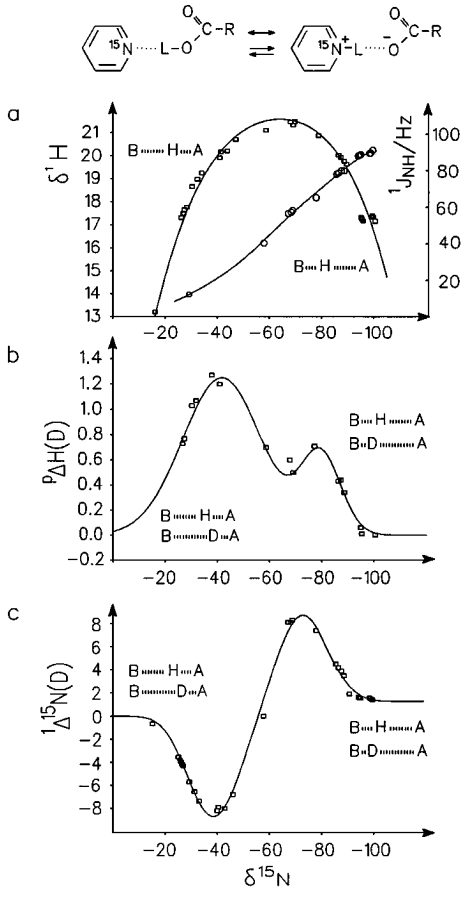

Figure 6. ^{1}H chemical shifts and $^{1}J_{^{1}H-^{15}N}$ coupling constants (a), primary H/D isotope effects on chemical shifts (b), and one-bond H/D isotope shifts on the ^{15}N atom of pyridine-^{15}N (c) in 1:1 complexes with carboxylic acids at low temperature. The curves were constructed from the data of Table 1 stemming from different acids and temperatures.

Isotope Effects on Chemical Shifts of 2:1 and 3:1 Complexes of Acetic Acid with Pyridine. As shown recently,[3o] carboxylic acids may form not only 1:1 complexes but also longer linear hydrogen-bonded chains with pyridine in freons at low temperature. Here we describe long-range isotope effects on chemical shifts of nuclei as far as two hydrogen bonds away

Table 1. Low-Temperature NMR Parameters of 1:1 Complexes of Protonated (AH) and Deuterated Acids (AD) with Pyridine-^{15}N (B) Dissolved in a 2:1 Mixture of $CDClF_2/CDF_3$[a]

AH	pK_a (25° C)	C_A (M)	C_B (M)	D	δ^{15}N(H)	δ^{15}N(D)	$^1\Delta^{15}$N(D)	δ^1H	δ^2H	$^p\Delta^1$H(D)	J (Hz)	T (K)
4-*tert*-butylphenol	>10	0.015	0.018	80	−16.16	−15.49	−0.67	13.2			0	117
acetic acid	4.75	0.037	0.07	35	−27.14	−23.19	−3.95	17.51			0	115.5
					−26.84	−23.02	−3.82	17.47			0	117.6
					−26.17	−22.62	−3.55	17.31			0	125.6
		0.034	0.02	42	−27.91	−23.62	−4.29				0	107.2
		0.08	0.04	46	−27.37	−23.26	−4.11	17.65			0	110.5
		0.05	0.03	50	−28.37	−24.0	−4.37	17.76			0	102
		0.05	0.06	80	−27.4*			17.57	16.80	0.77	0	110.6
					−26.8*			17.45	16.72	0.73	0	117
o-toluic acid	3.91	0.028	0.033	80	−34.06	−26.7	−7.36	19.24			un.	105.3
					−32.35	−25.8	−6.55	18.97			un.	113.6
					−30.35	−24.66	−5.69	18.65			un.	124.8
					−30.35			18.68	17.65	1.03	12	124.5
					−31.9*			18.91	17.84	1.07	13.4	116.3
3-bromopropionic acid	3.99	0.013	0.02	64	−41.0	−32.8	−8.2	19.9	18.7	1.2	un.	108.7
					−43.9	−35.9	−8	20.2			un.	100
benzoic acid	4.19	0.033	0.035	60	−47.16	−40.3	−6.8	20.7			un.	104.2
					−41.5	−33.6	−7.9	20.16			un.	115.4
					−37.9*			19.87	18.60	1.27	un.	122.6
formic acid	3.75	0.015	0.021	70	−58.8	−58.8(?)	≈0	21.10	20.4	0.7	40.5	104.5
2-thiophenecarboxylic acid	3.48	0.035	0.045	80	−69.2	−77.3	8.1	21.33	20.8	0.5	57.2	110
2-furoic acid	3.17	0.04	0.05	88	−69.8	−78.1	8.3	21.48			58.1	110.2
					−68.2	−76.2	8.1	21.47			56.7	115.3
					−67.9*			21.43	20.8	0.6	54	116.3
chloroacetic acid	2.85	0.021	0.023	65	−77.4*			20.94	20.23	0.71	64.1	116.6
		0.066	0.08	52	−78.9	−86.3	7.4	20.87			65.2	109.9
dichloroacetic	1.48	0.03	0.03	83	−86.5	−90.0	4.5	20.01	19.57	0.43	77.8	148
acid					−87.4	−91.6	4.2	19.92	19.48	0.44	78.5	137.7
					−88.7	−92.6	3.9	19.74	19.39	0.34	79.6	119
					−89.6	−93.1	3.5	19.63			79.7	103.6
HCl	<1	0.034	0.034	40	−95.1	−96.75	1.64	17.32			88.24	133.5
					−95.5	−97.1	1.60	17.25			88.46	124
					−95.9	−97.5	1.57	17.17			88.66	113
				74	−91.58	−93.5	1.92					202.7
				30				17.58	17.48	0.10	82.7	168
								17.48	17.41	0.07	87.1	158
								17.42	17.33	0.09	87.7	147
					−95.0*			17.34	17.28	0.06	87.4	137
					−95.4*			17.26	17.25	0.01	88.1	126
HNO_3	<1	0.02	0.02	70	−99.36	−100.94	1.58	17.39			89.3	144.5
					−99.70	−101.22	1.52	17.32			89.3	134.1
					−100.46	−101.89	1.43	17.16	17.1	≈0	90.8	112.0

[a] $C_A = C_{AH} + C_{AD}$: total acid concentration in mol L^{-1} (M); C_B: total pyridine concentration in mol L^{-1} (M); D: deuterium fraction in the mobile hydron sites; δ^{15}N(H), δ^{15}N(D): pyridine ^{15}N chemical shifts of the protonated and the deuterated 1:1 complexes in the pyridine ppm-scale; $^1\Delta^{15}N(D) = \delta^{15}N(H) - \delta^{15}N(D)$, δ^1H and δ^2H: chemical shifts of the H-bond proton and deuteron; $^p\Delta^1H(D) = \delta^1H - \delta^2H$; J: scalar coupling constant between ^{1}H and ^{15}N; T: temperature, un.: unresolved; *: result of extrapolation. The pK_a values were taken from ref 17.

from the isotopic substitution site. Figure 7a shows a low-temperature ^{15}N NMR spectrum of a mixture of acetic acid and pyridine in $CDClF_2/CDF_3$ (2:1). We observe three signals which were assigned previously[3o] to linear complexes of the type AHB, AHAHB, and AHAHAHB, as indicated at the top of Figure 7. The corresponding ^{1}H NMR spectrum with the assignments of all hydrogen bond protons is shown in Figure 7d. The $^1J_{^1H-^{15}N}$ coupling constants and the proton and nitrogen chemical shifts indicate a gradual proton transfer to pyridine due to an increase of the acidity or proton-donating power of acetic acid clusters in the order of AH < AHAH < AHAHAH. Either a fast intramolecular rearrangement shown at the top of Figure 7 or a bifurcated hydrogen bond between $AHAHA^-$ and HB^+ renders the two OHO protons equivalent unless they exhibit the same intrinsic chemical shifts. Deuteration in the mobile proton sites leads to additional isotopic species assigned in Figure 7.

1:1 Complex. The one-bond shift $^1\Delta^{15}N(D) = \delta(AH\underline{B}) - \delta(AD\underline{B})$ is negative in the case of the molecular complex ALB, indicating that the proton is close to the oxygen. The situation resembles the case discussed in Figure 5a−c.

3:1 Complex. The isotope shift $^1\Delta^{15}N(D) = \delta(ALALAH\underline{B}) - \delta(ALALAD\underline{B})$ for the zwitterionic 3:1 complex is positive (Figure 7b,c), indicating that the pyridine is fully protonated. The situation is similar to the case discussed in Figure 5d. Isotopic substitution in the remote oxygen sites has no observable influence. Minimal effects are observed in the ^{1}H NMR spectra (Figure 7e,f). Successive deuteration in neighboring hydrogen bonds leads to small low-field shifts of the protons monitored. Therefore, any weakening of a neighboring hydrogen bond by substitution of H by D leads to a strengthening of the hydrogen bond containing the proton monitored, i.e. to an anticooperativity of both hydrogen bonds.

2:1 Complex. The effects of anharmonic coupling are greater in the 2:1 complex. The ^{15}N NMR spectra indicate different chemical shifts for the species AHAHB, AHADB, ADAHB, and ADADB. The assignment of Figure 7b,c was achieved without uncertainty by taking spectra at different deuterium fractions. There are two different positive hydrogen bond shifts $^1\Delta^{15}N(D) = \delta(AHAH\underline{B}) - \delta(AHAD\underline{B}) = 8.5$ ppm and $^1\Delta^{15}N(D) = \delta(ADAH\underline{B}) - \delta(ADAD\underline{B}) = 8.2$ ppm and two different negative five-bond shifts $^5\Delta^{15}N(D) = \delta(AHAH\underline{B}) -$

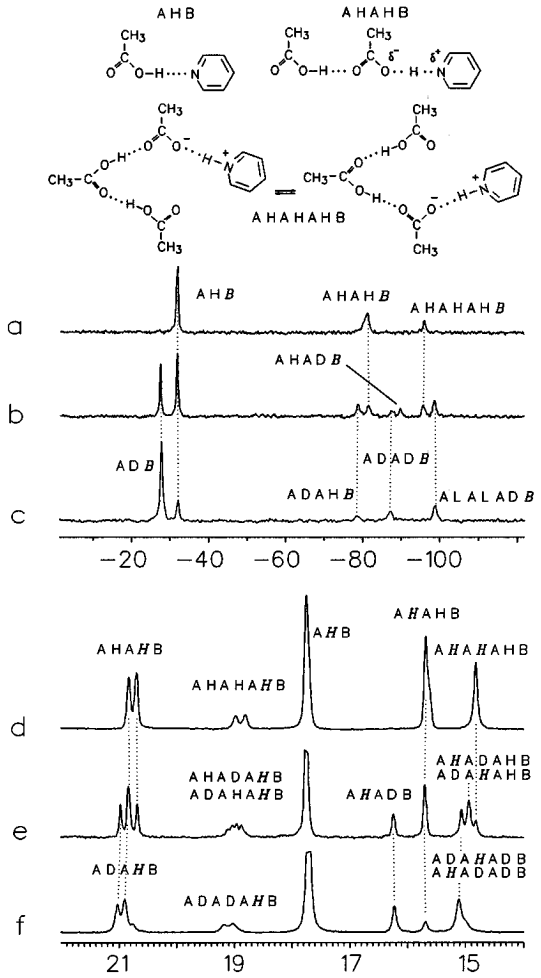

Figure 7. Low-temperature ^{15}N (a−c) and ^{1}H NMR spectra (d−f) (^{1}H Larmor frequency 500.13 MHz) of mixtures of acetic acid (AL, L = H, D) and pyridine-^{15}N (B) in a 2:1 mixture of $CDClF_2/CDF_3$ at various deuterium fractions D in the mobile proton sites. (a) 102 K, $D = 0$, $C_{AH} = 0.042$ M, $C_B = 0.026$ M. (b) 102 K, $D = 0.5$, $C_{AH} + C_{AD} = 0.05$ M, $C_B = 0.03$ M. (c) 105 K, $D = 0.85$, $C_{AH} + C_{AD} = 0.085$ M. $C_B = 0.05$ M. (d) As in a. (e) As in b. (f) As in c.

δ(ADAHB) = −2.8 ppm and $^{5}\Delta^{15}$N(D) = δ(AHADB) − δ(ADADB) = −2.3 ppm. The isotope effects on the ^{1}H NMR signals of the 2:1 complex are also noteworthy. The signal ALAHB is slightly shifted, and the signal AHALB is strongly shifted to low field by deuteration of the neighboring hydrogen bond, i.e. $^{4}\Delta$H(D) = δ(AHAHB) − δ(ADAHB) = 0.15 ppm and $^{4}\Delta$H(D) = δ(AHAHB) − δ(AHADB) = 0.54 ppm.

Discussion

We have described H/D isotope effects on the chemical shifts of low-barrier hydrogen-bonded 1:1 complexes between acids AL (L = H, D) and a base B (pyridine-^{15}N) in the liquid state at low temperatures, as a function of the proton-donating power of the acid employed. The observation that the spectral parameters obtained are independent of concentration indicates that complications arising from a possible aggregation especially of the zwitterionic complexes can be neglected in good approximation. It is interesting that all chemical shift values of Figure 6 are located on master curves, independent of the type of acid chosen or on temperature.

Although extended theoretical work will be necessary in order to give a quantitative description of the data obtained, we will try to give a tentative, qualitative explanation based on some simple assumptions. Firstly, we note that the plot of chemical

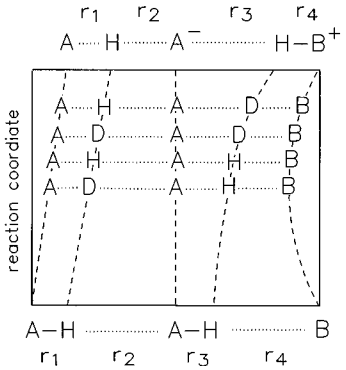

Figure 8. Average hydron (proton and deuteron) locations (schematically) in the 2:1 complex between acetic acid and pyridine arising from the experiments shown in Figure 6.

shifts of the hydrogen bond proton δ^{1}H vs the nitrogen chemical shifts δ^{15}N (Figure 6a) qualitatively follows the plot of $\langle r_1+r_2\rangle$ vs $\langle r_1-r_2\rangle$ depicted in Figure 3. In other words, δ^{1}H is a monotonous function of the average distance $\langle r_1+r_2\rangle$ between A and B, and δ^{15}N of the proton transfer coordinate $\langle r_1-r_2\rangle$. The observation that δ^{1}H goes through a maximum at about 21 ppm at δ^{15}N = −60 ppm with respect to free pyridine (Figure 6a) then indicates a hydrogen bond contraction approximately at the midpoint of the proton transfer from A to B as depicted in Figures 3 and 4. As a consequence, the positive primary isotope effects $^{p}\Delta$H(D) of Figure 6b indicate an increase of the A···B distance upon deuteration on either side of the quasi-midpoint. At the quasi-midpoint itself there is a noticable drop of $^{p}\Delta$H(D). At this point, $^{1}\Delta^{15}$N(D) also changes its sign (Figure 6c) which is consistent with Figures 3 and 4: deuteration in the region of the molecular complex decreases $\langle r_1\rangle$ and increases $\langle r_2\rangle$; by contrast, in the case of the zwitterionic complex, the opposite is true.

As discussed in the General Section, the observation that $^{1}\Delta^{15}$N(D) = 0 (Figure 6c) and $^{p}\Delta$H(D) ≠ 0 (Figure 6b) at the quasi-midpoint could be explained by the presence of a barrier for the proton motion according to Figure 4a. On the other hand, the drop of $^{p}\Delta$H(D) may also be explained with a very small barrier according to Figure 4b as follows. In a disordered polar solvent there is a distribution of various differently solvated hydrogen complexes characterized by sligthly different average values $\langle r_1-r_2\rangle$. These solvent complexes interchange rapidly within the NMR time scale. If the center of the distribution is located at $\langle r_1-r_2\rangle \approx 0$, where $^{1}\Delta^{15}$N(D) = 0, complexes with positive and negative values of $^{1}\Delta^{15}$N(D) exchange rapidly, leading to a vanishing overall value of $^{1}\Delta^{15}$N(D). By contrast, $^{p}\Delta$H(D) is not averaged to zero; a value of zero would only be expected in the case of a very sharp distribution.

Finally, we would like to point out that the symmetry of the $^{1}\Delta^{15}$N(D) vs δ^{15}N curve in Figure 6c may arise from a compensation of two effects. If we identify ^{15}N with B in Figure 4, the increase of the distance $\langle r_2\rangle$ between ^{15}N and L is more pronounced in the molecular complex A−L···B, where $\langle r_2\rangle$ is large, as compared to the zwitterionic complex A^{-}···L−B^{+}, where $\langle r_2\rangle$ is small. On the other hand, δ^{15}N is more sensitive to changes of $\langle r_2\rangle$ when the latter is small, leading overall to the symmetric aspect of the curve in Figure 5c. The observation that the two maxima in the curve $^{p}\Delta$H(D) vs δ^{15}N are not of equal height should reflect larger changes of the A···B bond distance when the hydron is closer to oxygen than to nitrogen.

The complex influence of deuteration on the chemical shifts of the 2:1 complex of acetic acid with pyridine depicted in Figure 7 can be rationalized qualitatively in terms of the hydron transfer pathway of Figure 8. For simplification the brackets

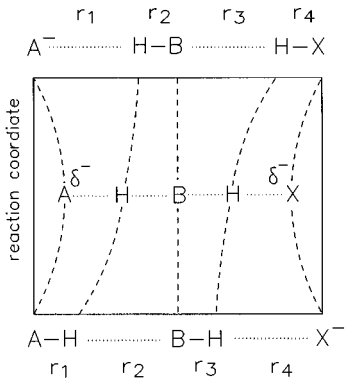

Figure 9. Hypothetical proton locations in a negatively charged hydrogen-bonded chain involving two low-barrier hydrogen bonds.

characterizing the average distances have been omitted. When a hydron shift from A toward B occurs, i.e. when r_4 is decreased, a positive charge is created at B and a negative charge at A. This will only lead to a contraction of the neighboring hydrogen bond, i.e. to a decrease of $r_1 + r_2$ because the acceptor capacity of A is increased but not to a substantial decrease of r_2. In other words, only A−L···A^-···L−B^+ is formed but not A^-···L−A···L−B^+, which would exhibit a larger Coulomb energy. The various isotopic species may be represented as various stages of the hydron transfer. Figure 8 was constructed as follows: the order of the ^{15}N chemical shifts indicates the degree of hydron transfer to B, i.e. the value of r_4. The proton chemical shifts indicate that the hydrogen bond to pyridine with the shortest value of $r_3 + r_4$ occurs in ADAHB. This information enables us firstly to place ADAHB on the proton transfer pathway of Figure 8 and then the other species, leading to a qualitative understanding of all isotope effects observed in terms of a cooperativity of the two hydrogen bonds: replacing H by D in the hydrogen bond to pyridine shifts the hydron more to pyridine but weakens this hydrogen bond; replacing D by H in the hydrogen bond between the two acetic acid residues strengthens this bond and shifts the other hydron further to pyridine.

There is another interesting but so far speculative conclusion from these results. Whereas in the neutral hydrogen bonded chain A−H···A−H···B a single proton transfer to B is preferred, accompanied by a strengthening of the second hydrogen bond, a chain exhibiting a negative charge A−H···B−H···X^- may behave in a different manner, as indicated in Figure 9. Here, the Coulombic interaction does not hinder a double proton transfer to A^-···H-B···H−X. Therefore, in the charge relay chains of serine proteases,[3] a negatively charged residue seems to be necessary in order to "relay" the charge during the course of the enzymatic reaction.

Conclusions

We have shown that low-temperature NMR spectroscopy using deuterated liquified gases as solvents enables the study of hydrogen-bonded complexes in the regime of slow hydrogen bond exchange and in particular the study of H/D isotope effects on chemical shifts of intermolecular hydrogen-bonded complexes and bond chains with low-barrier hydrogen bonds. So far, experiments were restricted to the study of intramolecular hydrogen bonds. Primary isotope effects could be observed not only on the chemical shifts of the hydrogen bond hydrons but also on those of the ^{15}N atom involved. Already, a qualitative discussion of the effects observed can lead to interesting novel insights into the properties of hydrogen bonds. In the future, one can expect a number of novel data which may be used for a more quantitative description. We are currently involved particularly in measuring isotopic H/D fractionation factors between different hydrogen-bonded sites from which we hope to obtain additional information concerning the potential curves of the proton motion in the complexes. In addition, we are studying in more detail the role of temperature, the solvent, and the solid state.

Acknowledgment. We thank the Stiftung Volkswagenwerk, Hannover, the fonds der Chemischen Industrie, Frankfurt, and the Russian foundation for fundamental Research (Project Nos. 93-03-5664 and 94-03-08533) for financial support.

JA953445+